Magnetic field effects on the NiO magnon spectra

J. Milano
CNEA, Centro Atómico Bariloche, (R8402AGP) San Carlos de Bariloche, Río Negro, Argentina

M. Grimsditch
Materials Science Division, Argonne National Laboratory, Argonne, Illinois 60439, USA
and CIC Nanogune, Donostia-San Sebastián, Spain

(Received 23 March 2009; revised manuscript received 28 November 2009; published 15 March 2010)

The effect of an external magnetic field on the eight antiferromagnetic resonance (AFMR) modes of NiO has been studied experimentally using Brillouin light scattering. The results are reproduced by a model that includes the effects of exchange, dipolar coupling, a small cubic anisotropy, and Zeeman terms. Magnetic fields up to 7 T were applied along several NiO crystalline directions. The agreement between theory and experiment provides additional proof that the model, recently introduced to explain the existence of the AFMR multiplet, is indeed valid. Deviations between simulations and experiments, together with a review of previously published results, indicate that large magnetostrictive effects are present in NiO.

DOI: 10.1103/PhysRevB.81.094415 PACS number(s): 75.30.Ds, 78.35.+c, 75.50.Ee

I. INTRODUCTION

Although nickel oxide is often considered to be a classical and simple example of an antiferromagnetic (AF) structure, it was recently shown[1] to exhibit more AF resonance (AFMR) modes than would be expected for a unit cell with two Ni atoms. In that study a model that includes exchange, dipolar coupling, and crystalline anisotropy indicated that the structure is actually composed of eight sublattices (four interpenetrating AF lattices) that lead to five distinct AFMR modes. By adjusting the model parameters the calculated mode frequencies were brought into agreement with the measured values.

The magnetic field dependence of the mode frequencies that we present here, provides not only a more complete understanding of NiO but also more firmly establishes the reliability of the parameters extracted from the model. The current interest in exchange bias phenomena, provides an additional incentive to ensure that we have an accurate microscopic picture of this important antiferromagnetic material.

It is well accepted that the AF structure of NiO consists of alternating ferromagnetically aligned (111) planes that are AF aligned with respect to each other (see Fig. 1).[2–4] The direction of spin alignment within each plane was the subject of some controversy but it is now generally accepted to be along $\langle 11\bar{2}\rangle$ directions.[4] The subtlety of antiferromagnetism in NiO can be emphasized (incorrectly as discussed below) by noting that, if the structure remained perfectly cubic, each Ni atom would have six ferromagnetic and six AF coupled nearest neighbors but, perplexingly, all 12 of them are crystallographically equivalent. Furthermore there is no combination of the two, lowest order, cubic anisotropies that leads to $[11\bar{2}]$ orientation of the spins. In this picture antiferromagnetism would have to rely on the small measured ($<10^{-3}$) trigonal distortion; this in turn, is then difficult to reconcile with its high Néel temperature.

Related to these structural issues there are also aspects of the magnetic normal modes, especially in the long-wavelength limit, that were not well understood. Two AFMR modes are observed at low temperatures via Raman scattering,[5,6] Brillouin scattering shows a central peak that vanishes at the Néel temperature (T_N),[7] and infrared absorption[8,9] shows a mode consistent with Raman-scattering results. Since a number of theoretical treatments[10,11] predict at most two AFMR modes, the "extra" modes have been ascribed to surface effects, grain size, or have been left unexplained. Further confusing the issue is an inelastic neutron-scattering[4] study, which together with its theoretical interpretation, indicates the existence of four zone-center modes whose frequencies are not consistent with the Raman or IR data. It was shown many decades ago by Kaplan,[12] Keffer and O'Sullivan,[13] and Yamada[14] that the structural aspects can be understood by including magnetic dipolar interactions between atoms. This contribution, presumably because of the complexity of including it into theoretical formalisms appears to have been replaced with an anisotropy in most subsequent treatments of the problem.[4,10,11] Loudon and Pincus[15] did show that in a two-sublattice model the inclusion of dipolar interactions has no effect on the frequency of the zero wave-vector magnons but does affect the finite wavelength magnons. Also, although dipolar terms were included in a theoretical description of small NiO particles,[16] when comparing the theory with experimental results, the dipolar terms were neglected in favor of an anisotropy.

In a previous work[1] we developed a model for the long-wavelength magnetic excitations that was based only on su-

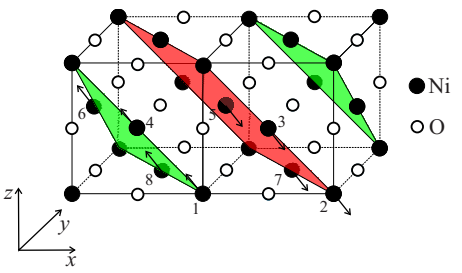

FIG. 1. (Color online) Schematic view of the crystalline and magnetic structure of NiO.

perexchange between Ni atoms, magnetic dipole-dipole interactions, and a small cubic anisotropy. Consistent with Refs. 12–14, the model predicted the correct magnetic structure, viz. (111), AF sheets and the $[11\bar{2}]$ spin orientation. It also predicts eight AFMR modes, three of which are doubly degenerate. Three of these five frequencies are consistent with the previously reported Raman doublet,[5,6] and with the central peak (zero frequency) observed by Brillouin scattering.[7] The two missing modes were found in the Brillouin scattering experiments reported in Ref. 1.

In this paper we report on the magnetic field dependence of the AFMR modes. Experimentally Brillouin spectra were recorded with applied magnetic fields up to 7 T. Theoretically the effects of an applied field were included into the same model used in Ref. 1.

II. MODEL

Hutchings and Samuelsen[4] have shown that the dominant interaction in NiO is the superexchange between next-nearest-neighbor Ni atoms (see Fig. 1). This finding is consistent with the fact that these atoms are "bonded" via a single p orbital of an oxygen atom. If this were the only interaction it would lead to four, uncoupled AF lattices. By defining the simple-cubic Ni lattices with the origins at (in units of the lattice parameter a): $o_1=(0,0,0)$, $o_2=(1,0,0)$, $o_3=(1/2,1/2,0)$, $o_4=(3/2,1/2,0)$, $o_5=(1/2,0,1/2)$, $o_6=(3/2,0,1/2)$, $o_7=(0,1/2,1/2)$, and $o_8=(1,1/2,1/2)$, it is easy to see (Fig. 1) that the superexchange couples only sublattices 1 and 2, 3 and 4, 5 and 6, and 7 and 8. The exchange energy can thus be written

$$E_{exch}=J(\mathbf{m}_1\cdot\mathbf{m}_2+\mathbf{m}_3\cdot\mathbf{m}_4+\mathbf{m}_5\cdot\mathbf{m}_6+\mathbf{m}_7\cdot\mathbf{m}_8), \quad (1)$$

where J is the coupling constant.

As described in Ref. 1 the dipolar interaction in our model is written

$$E_{dip}=D\sum_i\left[\sum_{j>i}m_iT_{ij}m_j\right]. \quad (2)$$

The strength of the interaction, D, is determined by the magnetic moment of each Ni atom and the lattice constant. $\mathbf{m}_i$ is the unit magnetization vector at each sublattice site i and it is defined as $\mathbf{m}_i=(\sin\theta_i\cos\phi_i,\sin\theta_i\sin\phi_i,\cos\theta_i)$. The tensors $\mathbf{T}_{ij}$ are derived as follows: all the atoms of a given sublattice are at vectors (h,j,k) (in units of a) from their origin; if $h+j+k$ is even, the vector, $\mathbf{r}_{pq}$, between two atoms on sublattices p and q is given by $\mathbf{r}_{pq}=o_p-o_q+(h,j,k)$. Performing the dipolar sums it is possible to show that

$$\mathbf{T}_{pq}=\mathbf{T}_{qp},$$

$$\mathbf{T}_{jj}=0,$$

and for two sublattices on the same AF lattice, $\mathbf{T}_{pq}=0$ (i.e., $\mathbf{T}_{12}=\mathbf{T}_{34}=\mathbf{T}_{56}=\mathbf{T}_{78}=0$).[1] The other tensors are of the form

$$\mathbf{T}_{13}=\begin{pmatrix}e & b & 0\\ b & e & 0\\ 0 & 0 & c\end{pmatrix}. \quad (3)$$

The remaining nonzero tensors are given explicitly in Ref. 1. The values of b, c, and e are 7.23, −4.32, and 2.17, respectively.

As concluded in earlier works[12–14] the dipolar energy couples the four AF lattices and leads to the ground state of AF-coupled ferromagnetically aligned (111) planes. It does not, however, align the spins along any axis within this plane.

In order for the model to yield the measured spin alignment it is necessary to introduce an additional, small, crystalline anisotropy. We chose to introduce the anisotropy via one of the usual cubic anisotropy terms, viz,

$$E_{ani}=K\sum_i(m_{ix}m_{iy}m_{iz})^2, \quad (4)$$

where K is the magnetocrystalline constant. In this case, it is negative favoring alignment along $\langle 111\rangle$ directions. Since the spins are confined (111) planes by the strong dipolar interaction, the effect of this anisotropy is to align the spins close to a $[11\bar{2}]$ direction in the plane but it has only a small effect on the out-of-plane orientation.

In this work we introduce an external magnetic field, which interacts with each sublattice. It is modeled through a Zeeman term,

$$E_{zee}=-\mathbf{H}\cdot\sum_i\mathbf{m}_i. \quad (5)$$

The equilibrium values of the θ_i and ϕ_i are found by direct minimization of the free-energy density,

$$E=E_{dip}+E_{exch}+E_{ani}+E_{zee}. \quad (6)$$

Following Refs. 17 and 18 the frequencies of the modes are related to the eigenvalues of the matrix built from the second derivatives of the energy with respect to θ_i and ϕ_j $[E_{\theta(\phi)_i\theta(\phi)_j}$ in Eq. (7)] via $\omega_k=i\gamma d_k/M$, where γ is the gyromagnetic ratio (0.098 cm^{-1}/kOe for Ni),[19] M is the saturation magnetization of each of the eight sublattices ($M=\mu_B/a^3=128$ G) and d_k are the mentioned eigenvalues. The elements, $B_{n,m}$, of that matrix are

$$B_{2i-1,2j-1}=E_{\theta_i\phi_j}/\sin\theta_j,$$

$$B_{2i,2j-1}=E_{\phi_i\phi_j}/\sin\theta_i\sin\theta_j,$$

$$B_{2i,2j}=-E_{\phi_i\theta_j}/\sin\theta_i,$$

$$B_{2i-1,2j}=-E_{\theta_i\theta_j}. \quad (7)$$

In Ref. 1, with $H=0$ and by setting the constants $D=6.55\times10^4$ erg/cm^3, $J=5.59\times10^8$ erg/cm^3, and $K=-2\times10^5$ erg/cm^3 (these values are different from those we use in the present work, see explanation below), our calculated frequencies were $\omega=\{43.0,38.5,38.5,13.9,6.6,6.6,0.94,0.94\}$ cm^{-1}; which are

in good agreement with those measured for $H=0$.[1] The experimental results, however, were somewhat perplexing since the frequency of the 5 cm^{-1} line depends slightly on the scattering geometry, a fact not expected from the model.

Another confusing issue is related to the mode intensities. Based on conventional magneto-optics, the intensities are expected to be given by

$$I \propto |\boldsymbol{e}_i \cdot \boldsymbol{\Delta\varepsilon}_{ij} \cdot \boldsymbol{e}_s|^2, \tag{8}$$

where $\boldsymbol{e}_i$ and $\boldsymbol{e}_s$ are the polarization vectors of the incident and scattered light and $\boldsymbol{\Delta\varepsilon}_{ij}$ is the change in the dielectric tensor induced by the magnon. Including both linear and quadratic terms we have $\boldsymbol{\Delta\varepsilon}_{ij}=m_k\mathbf{K}_{ijk}+m_kM_l\mathbf{G}_{ijkl}$, which for a cubic system reduces to[20]

$$m_k\mathbf{K}_{ijk} = K\sum_i \begin{pmatrix} 0 & m_z^i & -m_y^i \\ -m_z^i & 0 & m_x^{ji} \\ m_y^{ji} & -m_x^i & 0 \end{pmatrix} \tag{9}$$

and

$$m_kM_l\mathbf{G}_{ijkl} = G_{11}\sum_i \begin{pmatrix} 2M_x^im_x^i & 0 & 0 \\ 0 & 2M_y^im_y^i & 0 \\ 0 & 0 & 2M_z^im_z^i \end{pmatrix} + G_{12}\sum_i \begin{pmatrix} 2(M_y^im_y^i+M_z^im_z^i) & 0 & 0 \\ 0 & 2(M_x^im_x^i+M_z^im_z^i) & 0 \\ 0 & 0 & 2(M_y^im_y^i+M_x^im_x^i) \end{pmatrix}$$
$$+ G_{44}\sum_i \begin{pmatrix} 0 & 2(M_x^im_y^i+M_y^im_x^i) & 2(M_x^im_z^i+M_z^im_x^i) \\ 2(M_x^im_y^i+M_y^im_x^i) & 0 & 2(M_z^im_y^i+M_y^im_z^i) \\ 2(M_x^im_z^i+M_z^im_x^i) & 2(M_z^im_y^i+M_y^im_z^i) & 0 \end{pmatrix}. \tag{10}$$

$M_{z(x,y)}^i$ is the $z(x,y)$-static component of the i-sublattice magnetization, and replacing $m_{z(x,y)}^i$ by the eigenvectors of each calculated mode, the intensities are obtained.

The confusion that ensues from the above calculations is that they predict that the 15 cm^{-1} mode should be inactive: clearly in contradiction with the results of Ref. 1 where the 15 cm^{-1} mode was weak but observable. Presumably another coupling mechanism must be responsible. The experimental observation of a presumably "inactive" mode and the dependence of one of the mode frequencies on scattering geometry provides additional reasons to perform the field dependence of the modes to test the internal consistency of the model.

III. EXPERIMENTAL SETUP

In order to perform measurements in a magnetic field we used a cryostat with a superconducting magnet that produced fields in the range 0–7 T. The use of a cryostat also allowed us to measure at low temperatures where the linewidths of the AFMR modes are narrower. The drawbacks of the cryostat are that it significantly reduces the collection solid angle compared to our earlier experiments and also limits the number of scattering geometries that could be implemented. The measurements we report here were all performed at 150 K chosen as a compromise between obtaining narrow linewidths and having measurable intensities. The scattering geometries that could be implemented in the Brillouin experiments were constrained to have the incident laser beam at 90° to the scattering direction. Brillouin magnon spectra were excited with 350 mW of 514.5 nm radiation from an Ar laser. A tandem Fabry-Perot interferometer was used for the experiments: two free spectral ranges, i.e., 17.2 and 20 cm^{-1} were used.

We used a thin (~200 μm), unsupported and {100}-oriented single-crystal NiO sample grown by chemical-vapor deposition prepared as detailed in Ref. 7. The two scattering geometries that we were able to implement are shown in Fig. 2; we label them as platelet and backscattering, respectively. (The second geometry is not the conventional backscattering geometry where both the incident (k_i) and scattered (k_s) directions are close to the surface normal. However, since both beams enter and exit from the same surface, we chose to use the same nomenclature.)

Because the applied field is along the direction of the scattered light, in the platelet geometry it is easy, by setting α to 45°, to obtain a field along the [110] direction for our sample. Data for a [111]-field direction was also obtained in

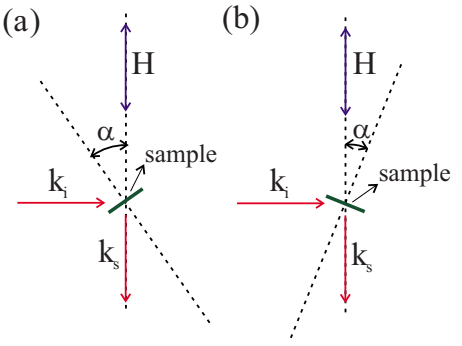

FIG. 2. (Color online) Schematic view of the (a) platelet and (b) backscattering geometries. k_i and k_s are the incident and scattered wave vectors, respectively. α is the angle between the surface normal and the applied field.

the platelet geometry of Fig. 2(a) with α set to 35°. Neither of the two geometries allowed us to measure with the applied field along [100]. Instead we measured as close as we could to the [100] direction by setting α to 23° in the geometry of Fig. 2(b). This is equivalent to applying the field along [12 5 0].

IV. RESULTS

Before applying the model to calculate the magnetic field dependence of the modes we reanalyzed our zero-field data to find the optimum parameters of the model. The three parameters of the model are the exchange (J), the dipolar coupling (D), and the anisotropy (K). In Ref. 1 we assumed that the constant D was not adjustable since its magnitude is fixed by the magnetic moment of the Ni atom. In that work we used J and K as the adjustable parameters. It turns out, however, that the magnetic moment of Ni atoms is temperature dependent[21] so it is possible for D to be smaller than the value we used earlier. In the present work we have re-evaluated the frequencies using the value 8.36×10^8 erg/cm^3 for J obtained from Ref. 4; thus leaving D and K as fitting parameters.

The value of K affects mainly the "central mode" and can be chosen over quite a wide range without noticeable changes to the other frequencies. Note, however, that it cannot be zero since it is necessary to align the spins close to $[11\bar{2}]$ directions and to bring the "zero-frequency" modes to into the 1 cm^{-1} range. With these constraints we chose $D=-4.4\times10^4$ erg/cm^3 and $K=9\times10^4$ erg/cm^3. The zero-field frequencies for these parameters are: $\omega = \{43.1, 38.4, 38.4, 14.1, 5.4, 5.4, 0.63, 0.63\}$ cm^{-1}.

In order to calculate the mode frequencies vs field it must be recognized that, even when the field is applied along a well-defined crystallographic direction, the existence of magnetic domains requires multiple calculations. Thus for a [100]-field direction, domains with $[11\bar{2}]$ or $[\bar{2}11]$ spin orientations are not equivalent. Similarly for a [111]-field direction the [211], $[1\bar{1}2]$, and $[11\bar{2}]$ spin directions are not equivalent. For a [110]-field direction the four inequivalent spin directions are [211], $[1\bar{1}\bar{2}]$, $[2\bar{1}1]$, and $[11\bar{2}]$. Ideally it would have been preferable to perform the experiments on a single-domain sample. Although the technique for obtaining single T domain samples using strain is known,[22] since this technique requires a stress along a ⟨111⟩ direction it was not suitable for our thin, [100]-oriented, platelet sample. We were also unable to obtain larger crystals of sufficient optical quality for the Brillouin experiments. Additionally, we note that a single T domain sample would only slightly simplify the analysis since even a single T (111) domain still has three possible spin orientations (S domains).

The mode frequencies for the [110] field direction are shown in Fig. 3. The lines are the model calculations and the symbols are experimental data. (The 15 cm^{-1} mode was not observed in this configuration). Since the [211] spin direction (dashed dotted line) has a soft mode at 0.55 T, it means that this spin orientation is unstable and rotates to one of the other stable orientations (see below). Therefore, only the other three orientations are plotted at higher fields. We note that the 15 cm^{-1} line, being nondegenerate does not split as fields are applied. The 5 cm^{-1} and the "central" peak, however, do split into a doublet for the $[2\bar{1}1]$ and $[11\bar{2}]$ spin directions while they remain a degenerate pair if the spin is along $[1\bar{1}\bar{2}]$. Although the experimental results agree very well with the calculations for the $[1\bar{1}\bar{2}]$ spin orientation, we can only speculate that the other spin orientations do not contribute either because of a strain-induced preferential T domain formation or given the existence of soft modes as a function of field, the field history could also determine which domains remain in the sample.

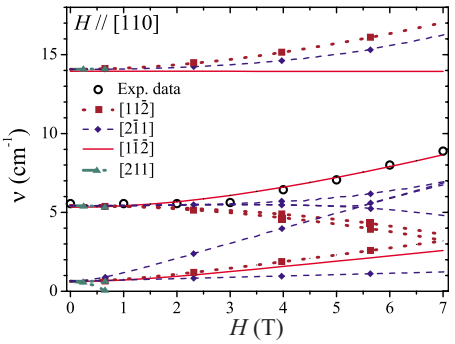

FIG. 3. (Color online) Calculated (lines) and measured (symbols) field dependence of the AFMR modes of NiO. The full, dashed, dotted, and dashed dotted lines correspond to the four inequivalent spin orientations relative to the [110]-field direction.

The field dependence of the polar angles of the four inequivalent ground-state spin orientations are shown in Fig. 4. This figure shows that, in general, the spins undergo only very small changes with respect to their zero-field directions. The exception is the [211] spin direction which, at 0.55 T—the same field at which one of the modes becomes soft [see Fig. 3], rotates to align along the $[1\bar{1}2]$ direction. On physical grounds this can be understood as follows. In an antiferromagnet with no anisotropy the lowest energy state is when the spins are aligned perpendicular to the applied field

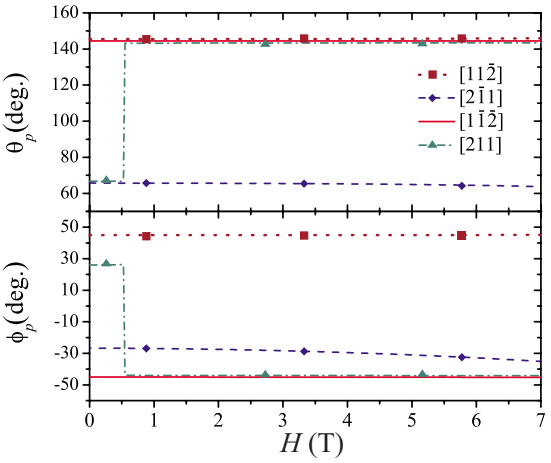

FIG. 4. (Color online) Calculated equilibrium angles as a function of a [110]-oriented applied field for the four inequivalent ground-state spin orientations.

TABLE I. Stability of spin orientations for the field directions investigated. H_{inv} indicates the field at which the instability occurs.

H direction	Spin direction at $H=0$	Stability	H_{inv} (T)	Spin direction above H_{inv}
[110]	$[11\bar{2}]$	Stable		
	$[2\bar{1}1]$	Stable		
	$[1\bar{1}\bar{2}]$	Stable		
	[211]	Unstable	0.55	$[1\bar{1}\bar{2}]$
[111]	$[11\bar{2}]$	Stable		
	[211]	Unstable	0.73	$[11\bar{2}]$
	$[1\bar{1}\bar{2}]$	Unstable	0.73	$[11\bar{2}]$
[100]	$[11\bar{2}]$	Unstable	6.80	$[01\bar{1}]$
	[211]	Unstable	1.15	$[11\bar{2}]$
[12 5 0]	$[1\bar{1}\bar{2}]$	Stable		
	$[1\bar{2}1]$	Stable		
	$[11\bar{2}]$	Unstable	4.25	$[1\bar{2}1]$
	[121]	Unstable	0.68	$[1\bar{2}1]$
	$[2\bar{1}1]$	Unstable	1.38	$[1\bar{2}1]$
	[211]	Unstable	0.60	$[1\bar{1}\bar{2}]$

so that a slight canting can reduce the Zeeman contribution to the energy. In this case the [211] direction is the one most parallel to the field (i.e., the most unstable) so that when the Zeeman energy is sufficient to overcome the anisotropy barrier the spins rotate to the direction that is perpendicular to the field, viz, to the $[1\bar{1}2]$ direction. It is interesting to note in Fig. 3 that both $[11\bar{2}]$ and $[2\bar{1}1]$ spin directions exhibit a softening of one mode that extrapolate to zero above 7 T. Based on the preceding arguments one can conjecture that when they do reach zero frequency the corresponding spins will also rotate to align along the most stable $[1\bar{1}2]$ direction perpendicular to the applied field. In Table I we have summarized the range of stability of the four spin directions for this direction of the applied field.

For a field along [111] the results are presented in Fig. 5. Again the three lines—full, dashed, and dotted—correspond to the three inequivalent spin directions. The calculations show that for this field direction domains with the spins along [211] and $[1\bar{1}2]$ have a mode that becomes soft at 0.73 T. Since this means that the domains are unstable and will reorient themselves into one of the other stable domains, we show no data for these orientations at higher fields. The frequencies for the single remaining stable spin direction, $[11\bar{2}]$, show no splitting of the degeneracy of either the 5 cm^{-1} or the central mode. Interestingly the calculations show that there is a mode crossing between the two lowest modes at about 6 T. The experimental results are consistent with a mode crossing around 4.5 T. However, while the model shows that the modes cross with no interaction, the experimental results are more indicative of a strong coupling between the modes that leads to the typical "repulsion" as they become close in frequency. Whatever causes the coupling is clearly not included in our model. The reorientation behaviors of the spin ground states for this field direction are listed in Table I.

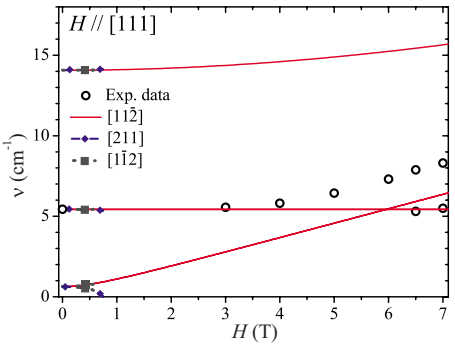

FIG. 5. (Color online) Calculated (lines) and measured (symbols) field dependence of the AFMR modes of NiO. The full, dashed, and dotted lines correspond to the three inequivalent spin orientations relative to the [111]-field direction.

In Fig. 6 we show the calculated (lines) and measured (symbols) frequencies for a field applied along [12 5 0], viz, as close as we could to [100]. For this direction of the field there are six inequivalent spin directions. Four of the six become unstable at fields below 4.25 T. For clarity, we have plotted only the frequencies for the two stable directions. The full and dashed lines represent the two stable inequivalent spin directions. Note that the doubly degenerate modes at around 1 and 5 cm^{-1} split into two modes at finite fields. We also stress, that as reported in our earlier work[1] the mode close to 5 cm^{-1} (i.e., at 4.5 cm^{-1}) is lower than in Figs. 3 and 5 (viz, 5.5 cm^{-1}). This effect remains unexplained and will be discussed in the next section. It should be noted, however, that the simulations correctly account for the small increases in the frequency of both modes as the field increases. Table I summarizes the stability regions of the various spin orientations.

Although we do not have experimental data for a field applied along [100] we present our calculated results in Fig. 7. The large differences between these results and those in Fig. 6 show that the field behavior of the modes is very strongly dependent on the direction of the applied field. In

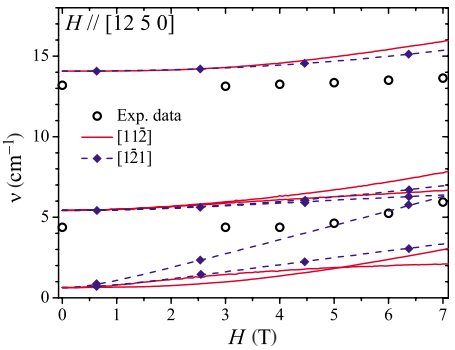

FIG. 6. (Color online) Calculated (lines) and measured (symbols) field dependence of the AFMR modes of NiO. The full and dashed lines correspond to the two inequivalent spin orientations relative to the [12 5 0] field direction, which remains stable up to 7 T.

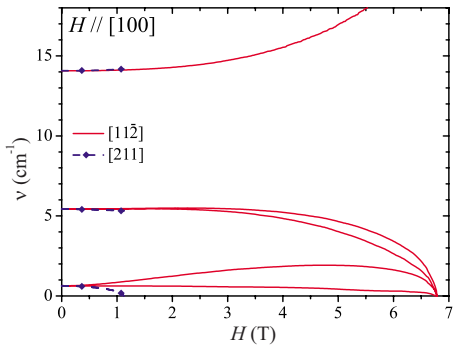

FIG. 7. (Color online) Calculated field dependence of the AFMR modes of NiO. The full and dashed lines correspond to the two inequivalent spin orientations relative to the [100]-field direction.

this context in the comparison made between the calculations and the experimental results in Figs. 3–6, one should also keep in mind that uncertainties in the crystal orientation during the measurements could also account for some of the discrepancies. The behavior for this direction of field is particularly interesting since above 6.8 T all ⟨112⟩ spin directions are unstable and they are reoriented along the [01$\bar{1}$]: perpendicular to the applied field as expected from the simple arguments presented earlier.

V. DISCUSSION

The field dependence of AFMR modes of NiO were measured up to 7 T for various field directions. The results are compared with, and found to be consistent with, the model of the magnetic structure of NiO presented in Ref. 1.

The small changes in the frequency of the AMFR modes of NiO measured here are consistent with the model developed in Ref. 1 and generalized here to include the effects of an applied field. Although our results do not allow the parameters of the model to be further refined, they do provide a valuable confirmation that the model does indeed capture the fundamental aspects of the magnetic normal modes of NiO. Numerous small differences between the experiments and modeling persist and are presumably due to shortcomings of the model. One can envision improving the model by adding additional exchange terms, including the variations in Zeeman energy due to the temperature dependence of the Ni moment and/or additional anisotropies. There are two reasons why implementing those changes is not likely to be particularly useful: the uncertainties in the experimental data are likely to preclude determining if any of the additional parameters are physically significant or simply a mathematical artifact of adding additional fitting parameters. Second neither of the two above-mentioned changes would explain either the dependence of the frequencies on scattering geometry nor the inability of magneto-optics to account for the observation of certain modes.

We believe that there is now sufficient evidence to infer that a magnetostrictive effects are responsible for most of the unexplained effects. We summarize them as follows. (1) In the Brillouin spectra in Ref. 7 there appears to be a very clear indication of a Fano-type interaction between some of the phonon peaks and the broad magnetic central peak. (We recall that Fano interactions occur when a discrete mode lies within, and couples to, a continuum background.[23] It typically leads to a peak-dip structure in the spectra.) (2) Two values for the elastic constant C_{11} were reported in Ref. 7 obtained from two different scattering geometries. The discrepancy disappeared above the Neel temperature. (3) The frequency of the mode at 5 cm^{-1} also depends on the scattering geometry, presumably, due to the change, either magnitude or direction, of the magnon probed. (4) Magneto-optic effects do not account for the observed intensities of the magnon peaks. (5) There is probably a mode coupling between AFMR modes (Fig. 5) that could be explained by a strain-induced coupling.

At present it is not clear how to introduce magnetostrictive terms into our model. It is, however, interesting to speculate that since the effects appear to be quite large, if a single crystal of NiO could be produced with a single domain, both for the chosen (111) AF plane as well as a single [112] spin orientation, it might turn out to be a material with very strong, and perhaps useful, piezomagneto- or magneto-optic properties.

This study also provides a methodology for obtaining a NiO sample that is truly single domain. First, following the procedure using strain described in Ref. 22, a single-crystal NiO sample with a single T domain (and three S domains) is fabricated. Second, by applying a field larger than 1.2 T along a [100] direction, above which only one stable spin-orientation remains, will produce a truly single-domain crystal of NiO.

ACKNOWLEDGMENTS

Work at ANL was supported by the U.S. DOE, Basic Energy Sciences, Materials Sciences under Contract No. W-31-109-ENG-38. Work at CNEA was partially funded by PIP 6016. J.M. is member of CONICET Argentina. M.G. acknowledges support from the Ikerbasque foundation.

[1] J. Milano, L. B. Steren, and M. Grimsditch, Phys. Rev. Lett. **93**, 077601 (2004).
[2] W. L. Roth, Phys. Rev. **110**, 1333 (1958).
[3] H. Kondoh and T. Takeda, J. Phys. Soc. Jpn. **19**, 2041 (1964).
[4] M. T. Hutchings and E. J. Samuelsen, Phys. Rev. B **6**, 3447 (1972).
[5] D. J. Lockwood, Fiz. Nizk. Temp. **18** (Suppl. 1), 165 (1992); D. J. Lockwood, M. G. Cottam, and J. Baskey, J. Magn. Magn. Mater. **104-107**, 1053 (1992).
[6] M. Grimsditch, L. E. McNeil, and D. J. Lockwood, Phys. Rev. B

58, 14462 (1998).
[7] M. Grimsditch, S. Kumar, and R. Goldman, J. Magn. Magn. Mater. **129**, 327 (1994).
[8] A. J. Sievers and M. Tinkham, Phys. Rev. **129**, 1566 (1963).
[9] V. V. Pishko, S. Gnatchenko, V. Tsapenko, R. H. Kodama, and S. Makhlouf, J. Appl. Phys. **93**, 7382 (2003).
[10] M. G. Cottam and A. Latiff, J. Phys. C **12**, 105 (1979).
[11] A. Stevens, J. Phys. C **5**, 1859 (1972).
[12] J. Kaplan, J. Chem. Phys. **22**, 1709 (1954).
[13] F. Keffer and W. O'Sullivan, Phys. Rev. **108**, 637 (1957).
[14] T. Yamada, J. Phys. Soc. Jpn. **21**, 650 (1966); **21**, 664 (1966).
[15] R. Loudon and P. Pincus, Phys. Rev. **132**, 673 (1963).
[16] R. H. Kodama and A. E. Berkowitz, Phys. Rev. B **59**, 6321 (1999).
[17] J. Smit and H. G. Beljers, Philips Res. Rep. **10**, 113 (1955).
[18] Z. Zhang, L. Zhou, P. E. Wigen, and K. Ounadjela, Phys. Rev. B **50**, 6094 (1994).
[19] E. P. Wohlfahrt, *Ferromagnetic Materials* (North-Holland, Amsterdam, 1980).
[20] W. Wettling, M. G. Cottam, and J. R. Sandercock, J. Phys. C **8**, 211 (1975).
[21] H. A. Alperin, J. Phys. Soc. Jpn. **17** Suppl. B-III, 12 (1962).
[22] G. Srinivasan and Mohindar S. Seehra, Phys. Rev. B **29**, 6295 (1984).
[23] G. Abstreiter, M. Cardona, and A. Pinczuk, *Light Scattering in Solids IV*, Topics in Applied Physics Vol. 54 (Springer, Berlin, 1984), p. 5.